Korean Chem. Eng. Res., 54(5), 659-664 (2016)
http://dx.doi.org/10.9713/kcer.2016.54.5.659
PISSN 0304-128X, EISSN 2233-9558

Migration of Alkali and Alkaline Earth Metallic Species and Structure Analysis of Sawdust Pyrolysis Biochar

Yijun Zhao, Dongdong Feng, Yu Zhang, Wenbo Tang, Shun Meng, Yangzhou Guo and Shaozeng Sun†

School of Energy Science and Engineering, Harbin Institute of Technology, Harbin 150001, PR China
(Received 13 March 2016; Received in revised form 7 June 2016; accepted 16 June 2016)

Abstract – In order to resolve the AAEM species migration routes and the interaction relationship between biochar structure and AAEM species during biomass pyrolysis, experiments were performed in an entrained flow reactor with N_2 at 500~900 °C. ICP-AES, XPS and SEM-EDX were used to examine content and distribution of AAEM species and the physicochemical structures of biochar. The results show that at 500~700 °C, the precipitation rate of AAEM species is relatively high. At high temperature (>700 °C), the AAEM species continue to migrate from interior to exterior, but little precipitation from biochar surface. And the migration of AAEM species is mainly realized by the C-O bond as the carrier medium. The AAEM species on biochar surface are mainly Na, Mg and Ca (<700 °C), while changing to K, Mg and Ca (≥700 °C). From 500 °C to 900 °C, the biochar particle morphology gradually changes from fibers to porous structures, finally to molten particles. At 700~900 °C, Ca element is obviously enriched on the molten edge of the biochar porous structures.

Key words: Pyrolysis, AAEM species, Biochar structure, C-O bond, Particle morphology

1. Introduction

Pyrolysis is an important and common process during biomass thermochemical conversion [1,2]. The physicochemical properties of samples are particularly important during the pyrolysis process. The transformation of char structures, such as the surface functional groups [3,4] and aromatic ring system [5] during pyrolysis have been investigated before. And the alkali and alkaline earth metal (AAEM) species are located in the interior and surface of biomass carbon matrix, which affects the biomass pyrolysis process. Many researchers have investigated the influence of AAEM species on the light hydrocarbons [6-9], oxygen-containing species [9-11], char [7,8,12,13] and tar [6,8-10] during biomass pyrolysis using a variety of reactors. The function mechanism of AAEM species was reported about the total amount [14], inorganic/organic chemical forms [15] and some direct aspects about AAEM species. However, the migration paths of AAEM species from the interior to exterior of biomass samples, as well as the precipitation process of AAEM species from the surface of biochar (i.e., at the gas-solid interface) have not been presented in the relevant reports. Meanwhile, the interaction mechanisms of AAEM migration and biochar structure transformation are still not clear.

To resolve the AAEM species migration routes and the interaction relationship between biochar structure and AAEM species during biomass pyrolysis, experiments were performed in an entrained flow reactor with N_2 at 500~900 °C. The physicochemical properties of pyrolysis biochar, including particle morphology, surface distribution of AAEM species, surface functional groups and the total amount of AAEM species were studied by scanning electron microscopy (SEM), energy-dispersive X-ray spectroscopy (EDX), X-ray photoelectron spectroscopy (XPS) and inductively coupled plasma atomic emission spectrometry (ICP-AES), respectively.

2. Experimental Section

2-1. Material preparation

Manchurian walnut sawdust (*Juglans mandshurica*), which is abundant in northeastern China, was used in the experiments. After being dried at 105 °C overnight, the samples were crushed further and sieved to a particle size of 0.15~0.25 mm. The entrained flow reactor and experimental process were described in detail in an earlier study [4], as shown in Fig. 1. Pyrolysis temperatures of 500 °C, 600 °C, 700 °C, 800 °C and 900 °C were investigated. After the reactor reached the target temperature and stabilized, the biomass particles were fed into the reactor at a rate of 1.0 g/min through the fuel feeder system. The biomass particles were introduced through a water-cooled probe to avoid release of volatiles before the particles reached the target temperature zone. Nitrogen gas at room temperature and flow rates of 8.00 L/min, 7.18 L/min, 6.33 L/min, 5.70 L/min and 5.28 L/min were used for the reaction temperatures of 500 °C, 600 °C, 700 °C, 800 °C and 900 °C, respectively, to maintain a residence time of 4.2 s at the different pyrolysis temperatures. The pyrolysis biochar samples were achieved from the bottom sampling system.

† To whom correspondence should be addressed.
E-mail: sunsz@hit.edu.cn

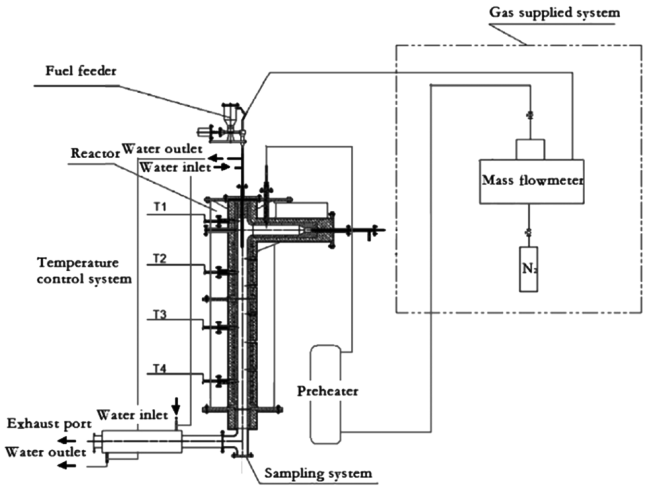

Fig. 1. Schematic diagram of the entrained flow reactor.

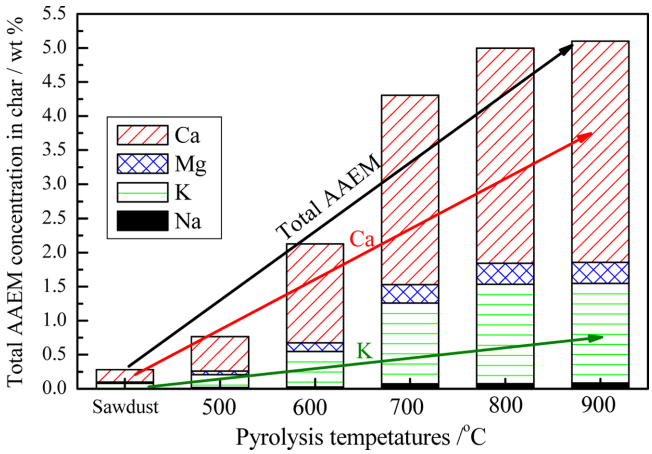

Fig. 2. Total concentration of AAEM species of biochar.

2-2. Analysis methods

XPS analysis of pyrolysis biochar was performed using a K-Alpha spectrometer (Thermo Fisher Scientific) with monochromatic Al Ka X-rays at 1486.6 eV. XPS data were corrected using the maximum peak of the C1s binding energy of adventitious carbon corresponding to 284.6 eV.

The pyrolysis biochars were digested by a microwave digestion system (Ethos 1, Milestone, Sorisole, Italy). For the digestion, each sample (1.0 g) was digested in a 1:3:8 (v/v/v) mixture of 40% HF, 30% H_2O_2 and 65% HNO_3. The digestion was carried out at 200 °C for 45 min. The solvent residue was transferred to a 50-mL volumetric flask and made up to this volume with deionized water. The concentration of AAEM species in pyrolysis biochar was quantified by the inductively coupled plasma atomic emission spectrometry.

The biochar particle morphology, surface content and distribution of AAEM species were measured by the EVO18 scanning electron microscope with the energy dispersive X-ray spectrometer (Carl Zeiss, Germany).

The experimental tests were run three times to ensure that the error range was within 5% and the test results were from the average value.

3. Results and Discussion

3-1. Migration of alkali and alkaline earth metallic species

The total concentration of AAEM species in sawdust and pyrolysis biochar at different temperatures is shown in Fig. 2. The AAEM species have a considerable effect on biomass thermal transformation, which are acting as the catalytically active sites in biochar during the reaction [16]. The migration and precipitation of AAEM species in biomass samples mostly depend on the temperature. During the thermal transformation at 500~900 °C, the AAEM species in the sawdust are staying in a very active state. With the pyrolysis temperature increasing from 500 to 900 °C, the total concentration of AAEM species increased from 0.28% to 5.10%. This phenomenon can be explained as follows: the concentration of AAEM species in the pyrolysis biochar is closely related to the coupling effect of the precipitation and retention of AAEM species. Over the temperature range of 500~900 °C, the AAEM species have different rates of precipitation and evaporation. With rising pyrolysis temperature, the degree of precipitation gradually increases. However, volatiles (tar, light gas and so on) from the sawdust samples are formed and released into the bio-oil and gas phases, while most of the less-volatile inorganic species remains in the solid biochar phase, which increases the concentration of AAEM species in the pyrolysis biochar [17]. With the temperature ranging from 500 to 700 °C, the quality of the raw material rapidly decreases through the decomposition of lignin, cellulose and hemicellulose. The precipitation rate of AAEM species during this process is relatively high. From 500 to 700 °C, the content of Ca increases from 0.51% to 2.78% and that of K increased from 0.19% to 1.19%. The content of AAEM species changes markedly following pyrolysis at high temperature (>700 °C). The AAEM species form a volatile phase at such high temperature [14]. At 800 °C, the structure of biochar was basically formed, and the precipitation of volatile was almost complete. The AAEM species continued to migrate from the interior to the exterior of the structure, but there was little precipitation. Therefore, the relative concentrations of AAEM species in the samples pyrolyzed at 700~900 °C are similar. The content of K increased from 1.19% to 1.46%, that of Mg increased from 0.27% to 0.31%, and that of Ca increased from 2.78% to 3.25%. The content of K and Na was relatively low, which indicates that their precipitation rate was relatively high. The relative content of Ca and Mg was substantially increased (especially Ca) compared with those in the sawdust. Current research shows that a high temperature (<950 °C) as well as the volatile-char interactions facilitate the migration of K and Na more than that of Ca and Mg [18]. Compared with K and Na linked to the sawdust through a single bond, Ca and Mg elements, with their two bonds connected to the char structure, are more stable.

XPS analysis was used to evaluate the surface characteristics of elements in biochar. The element state was analyzed through the number of escaped electrons from the char surface at a depth of 1~10 nm.

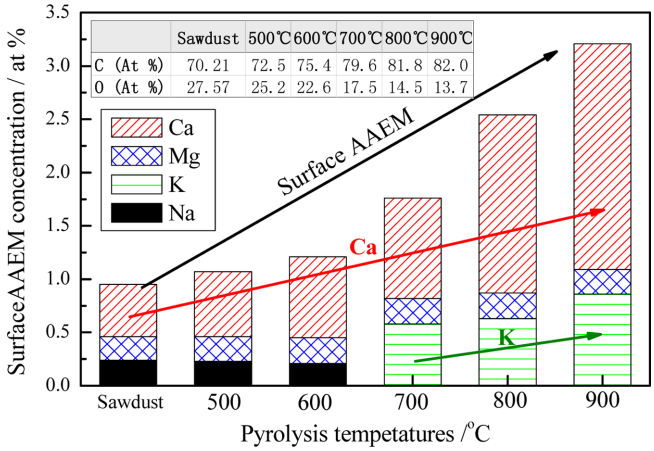

Fig. 3. Surface concentration of AAEM species of biochar.

The transformation of the main carbon and oxygen functional groups on the char surface determined by XPS analysis has been described in detail elsewhere [4]. During pyrolysis, the decrease of oxygen content and consumption of char occurs along with the migration of AAEM species from interior to exterior of the particles, as well as precipitation from the surface of biochar. As shown in Fig. 3, with pyrolysis temperature increasing from 500 to 900 °C, the relative content of C atom gradually increased, while that of the O atom gradually decreased. As the investigation before [4], the change of C-O bonds is the main transformation of oxygen-containing char structure during pyrolysis. As shown in Fig. 4, with the temperature rising, the content of C-O bonds decreased substantially, while the content of C=O and O=C-O bonds was relatively stable. In fact, during the thermal conservation, the C=O and O=C-O bonds were also consumed, while the content of C=O and O=C-O bonds remained stable because of the addition reaction of C-O. In the internal and external structures of char, the AAEM species are connected to the carbon matrix (CM-O-AAEM) via O atom [19]. The transformation and migration of AAEM species are realized through O as a transfer medium. Combined with the relevant data analysis of this paper, we can get the information that during the transformation of the C-O bond,

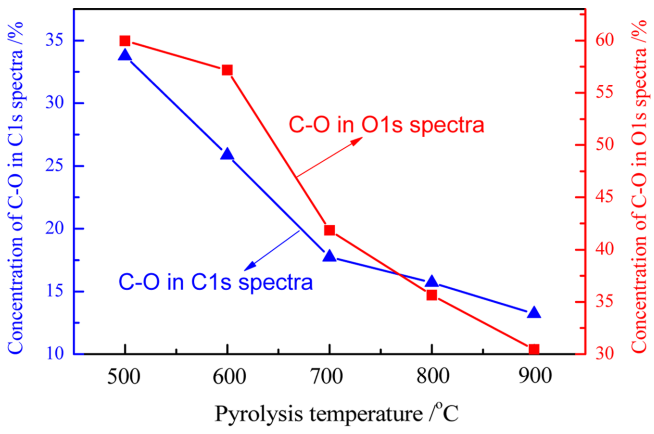

Fig. 4. Relative content of C-O functional group in the XPS C1s (a) and O1s (b) spectra.

the AAEM species migrate from inside the biochar structure to its surface, and eventually separate out from the gas-solid interface. The C-O bond plays a vital role as a carrier medium for this process.

As shown in Fig. 3, with the pyrolysis temperature increasing from 500 to 900 °C, the content of Mg on the surface of biochar particles remains unchanged at about 0.23%. At lower temperature (<700 °C), the AAEM species on the char surface are mainly Na, Mg and Ca. The concentrations of Na and Mg are relatively stable and around 0.23%~0.24%. Meanwhile, the concentration of Ca element is increased from 0.49% in the raw sawdust to 0.61%. With the release of Na at the gas-solid interface, the Na in the internal char structure migrates to the char surface via the C-O bonds, which allows the Na content on the char surface to remain stable relatively. Because it is connected to the char structure by two bonds rather than one like Na, the surface Ca is more stable than Na; that is, the precipitation of Ca at the gas-solid interface is more difficult than that of Na, so there is a slight increase of Ca content. At 500 and 600 °C, K has no obvious distribution on the char surface. At higher pyrolysis temperature (≥700 °C), the AAEM species on the surface are mainly K, Mg and Ca. The concentration of Mg is relatively stable at about 0.24%. Conversely, the content of K and Ca increases considerably. The content of K increases from 0.58% at 700 °C to 0.86% at 900 °C, and that of Ca element increases from 0.94% at 700 °C to 2.12% at 900 °C. The content of Na is very low and its migration and precipitation are faster than those of K and Ca. Thus, Na is not obvious on the char surface. At low temperature, the concentration of Mg on the char surface remains constant. Meanwhile, the content of K and Ca gradually increases with pyrolysis temperature. The precipitation rate of K and Ca at the gas-solid interface is lower than that of migration from the interior to the exterior of the char structure. Thus, the content of K and Ca increases considerably in the samples pyrolyzed at higher temperature.

3-2. Biochar Morphology and Surface Distribution of AAEM Species

As shown in Fig. 5(a~i), the morphology of typical biochar particles along with the content and surface distribution of AAEM species determined by SEM-EDX analysis are presented. The red points in Fig. 5(b,d,f,h,j) indicate the AAEM species on the surface of samples. During pyrolysis, AAEM species with catalytic activity are only distributed on the surface of the pore structure of biochar because they are closely related to the gas phase. AAEM species exist in the raw biomass as salts and organic materials. They are evenly distributed in the carbon matrix of biomass at the atomic and molecular levels. The raw biomass and biochar samples prepared at low temperature contain numerous oxygen groups. Therefore, the AAEM species are connected with the char structure. This means that the AAEM species are still distributed inside the carbon matrix rather than on the surface of the pores. Thus, some AAEM species are inaccessible for catalysis. As the pyrolysis temperature increased, the content of oxygen in the char decreased and the graphitization degree of biochar increased. The AAEM species are forced to migrate from the carbon

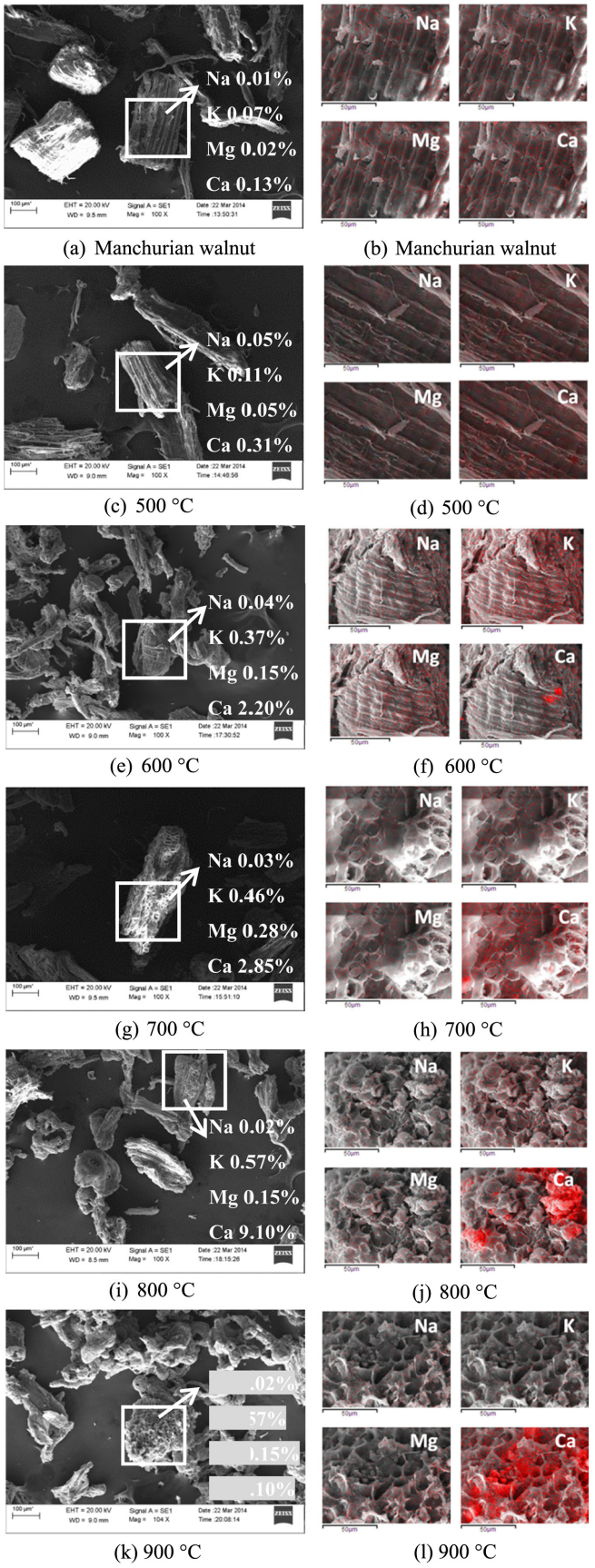

Fig. 5. (a,c,e,g,i,k) SEM image and surface AAEM species weight rate, (b,d,f,h,j) surface AAEM distribution of Manchurian walnut and 500~900 °C pyrolysis biochar.

matrix to the surface of the porous structure through a bond breaking and reforming process [18].

The area highlighted by the red rectangle in Fig. 5(a) shows the main structure of Manchurian walnut sawdust, which is fibers. This fiber structure is closely related to the growth mechanism of sawdust. The content of AAEM species in the fibrous structure of sawdust is low. These four elements are all evenly distributed on the surface of the sawdust particles as shown in Fig. 5(b). For the pyrolysis biochar at 500~600 °C, as shown in Fig. 5(c~f), the structure of biochar particle is still dominated by fibers. Because the evaporation of volatile is not complete, only the lateral deformation of fiber-shaped structures occurs under these conditions, so their structures are not uniform [20]. The structures contain some fibers that have separated from the main network. In addition, there is lateral expansion and volume contraction of the fiber structures. The AAEM species on the surface of these samples are still distributed uniformly. Compared with the sawdust, the content of surface AAEM species increases gradually. The surface weight rates of K and Ca increase from 0.07% and 0.13% to 0.37% and 2.20%, respectively. These results can be explained by the gradual migration of elemental Na and K to the surface of the carbon matrix during lateral deformation of the fibrous structure. Meanwhile, because of their connection to the carbon framework through two organic bonds, Ca and Mg are not clearly separated at the pore surface. There is some enrichment of Ca at local positions. The content of fibers decreases and the number of the pores increases obviously in the sample treated at 700 °C, as shown in Fig. 5(g~h). Compared with 600 °C, the pore structure develops into a honeycomb structure. The content of Ca in this porous structure also increases obviously. The formation of the porous structure at 700 °C results in precipitation of a large amount of AAEM species. Regarding the monovalent elements, Na and K are evenly distributed over the sample surface. Because of its two bonds with the carbon framework, the precipitation of elemental Mg is not obvious, and its distribution is still uniform. Because of the high content of Ca and its connection to the carbon structure via two bonds, the content of elemental Ca in the pore structures only increased at higher pyrolysis temperature. Fig. 5(i~j) reveals that the fiber structures have almost disappeared following pyrolysis at 800 °C, and are replaced by the highly porous structures. The tips of the hole walls in the porous structure have melted to varying degrees [21]. The content of Ca at these positions is obviously enriched (up to 9.1%). At such high temperature, the particle structure starts to collapse. Ca, Si and O form $CaSiO_3$, CaO and other stable Ca compounds. Relative to Mg in the equivalent reaction, the Gibbs free energy of Ca reacting with SiO_2 to generate $CaSiO_3$ is much smaller [22]. This means that $CaSiO_3$ is easier to produce than $MgSiO_3$. However, because $CaSiO_3$ does not easily precipitate, it stays trapped in the char, so there is less precipitation of Ca than Mg. Fig. 5(k~l) indicates that the melted structure of char particles has been transformed into the main structure following pyrolysis at 900 °C. When the pyrolysis temperature was 900 °C, the fibrous structure of sawdust basically disappeared, and the content of porous structure

also decreased. Ca in incomplete fusion sites is not completely covered, and there is some Ca enrichment at the sample surface. The Ca enrichment is the most obvious where the multipore structure begins to melt and Ca is not completely encapsulated. The biochar surface melts at high heating rate and high reaction temperature. In the molten state, the pore surface becomes smoother than that in the solid state [23]. The pore walls of the char particles are enriched with Ca, the results can be seen in the related reference [24]. In the formation process of biochar, a large number of surface oxygen functional groups provide attachment sites for organic AAEM species. AAEM elements such as Ca are bound through cross-linking to the large three-dimensional molecular structure of the char. This promotes the surface enrichment of Ca during the transformation process of biochar structure.

4. Conclusions

(1) At 500~700 °C, the precipitation rate of AAEM species during pyrolysis is relatively high. At high temperature (>700 °C), the AAEM species continue to migrate from interior to exterior, but little precipitation from biochar surface.

(2) The migration of AAEM species from interior to exterior of biomass particles during pyrolysis is mainly realized by the C-O bond as the carrier medium.

(3) The AAEM species on biochar surface are mainly Na, Mg and Ca elements at lower temperature (<700 °C), while they become K, Mg and Ca elements at higher temperature (≥700 °C).

(4) From 500 to 900 °C, the biochar particle morphology gradually changes from fibers to porous structures, finally to molten particles. At 700~900 °C, Ca element is obviously enriched on the molten edge of the biochar porous structures.

Acknowledgments

Financial support from the National Natural Science Foundation of China (Grant No. 51206037) and the National Natural Science Foundation Innovation Research Group Heat Transfer and Flow Control (Grant No. 51421063) is gratefully acknowledged.

References

1. Basu, P., *Biomass Gasification and Pyrolysis: Practical Design and Theory*. Academic press: 2010.
2. Sun, L. and Zhang, X., *Biomass Pyrolysis Gasification Principle and Technology*. Chemical Industry: 2013.
3. Lin, X., Wang, C., Ideta, K., Jin, M., Nishiyama, Y., Wang, Y., Yoon, S. and Mochida, I., "Insights into the Functional Group Transformation of a Chinese Brown Coal During Slow Pyrolysis by Combining Various Experiments," *Fuel*, **118**, 257-264(2014).
4. Zhao, Y., Feng, D., Zhang, Y., Huang, Y. and Sun, S., "Effect of Pyrolysis Temperature on Char Structure and Chemical Speciation of Alkali and Alkaline Earth Metallic Species in Biochar," *Fuel Processing Technology*, **141**, 54-60(2016).
5. Li, X., Hayashi, J. I. and Li, C. Z., "FT-Raman Spectroscopic Study of the Evolution of Char Structure During the Pyrolysis of a Victorian Brown Coal," *Journal of Clinical Pathology*, **2**(12), 1700-1707(1969).
6. Tyler, R. J. and Schafer, H. N. S., "Flash Pyrolysis of Coals: Influence of Cations on the Devolatilization Behaviour of Brown Coals," *Fuel*, **59**(7), 487-494(1980).
7. Tyler, R. J., "Flash Pyrolysis of Coals. 1. Devolatilization of a Victorian Brown Coal in a Small Fluidized-bed Reactor," *Fuel*, **58**(9), 680-686(1979).
8. Doolan, K. R., Mackie, J. C. and Tyler, R. J., "Coal Flash Pyrolysis: Secondary Cracking of Tar Vapours in the Range 870~2000 K," *Fuel*, **66**(4), 572-578(1987).
9. Doolan, K. R., Mackie, J. C., Mulcahy, M. F. R. and Tyler, R. J., "Kinetics of Rapid Pyrolysis and Hydropyrolysis of a Sub-bituminous Coal," *Symposium on Combustion*, **19**(1), 1131-1138(1982).
10. Solomon, P. R., Serio, M. A., Despande, G. V. and Kroo, E., "Cross-linking Reactions During Coal Conversion," *Energy Fuels*, **4**(1), 42-54(1990).
11. Wornat, M. J. and Nelson, P. F., "Oxygen-containing Gases from the Rapid Pyrolysis of a Brown Coal: The Effects of Ion-exchanged Calcium," *Symposium on Combustion*, **23**(1), 1239-1245(1991).
12. Best, P. E., Solomon, P. R., Serio, M. A., Suuberg, E. M., Mott, W. R. and Bassilakis, R., "Relationship Between Char Reactivity and Physical and Chemical Structural Features," *Prepr. Pap., Am. Chem. Soc., Div. Fuel Chem.; (United States)*, **32**, 4(1987).
13. Yeasmin, H., Mathews, J. F. and Ouyang, S., "Rapid Devolatilisation of Yallourn Brown Coal at High Pressures and Temperatures," *Fuel*, **78**(1), 11-24(1999).
14. Hanson, J., "Primary Release of Alkali and Alkaline Earth Metallic Species during the Pyrolysis of Pulverized Biomass," *Energy & Fuels*, **19**(5), 2164-2171(2005).
15. Jordan, C. A. and Akay, G., "Speciation and Distribution of Alkali, Alkali Earth Metals and Major Ash Forming Elements During Gasification of Fuel Cane Bagasse," *Fuel*, **91**(1), 253-263(2012).
16. Li, C.-Z., Sathe, C., Kershaw, J. and Pang, Y., "Fates and Roles of Alkali and Alkaline Earth Metals During the Pyrolysis of a Victorian Brown Coal," *Fuel*, **79**(3), 427-438(2000).
17. Liu, W. J., Jiang, H., and Yu, H. Q., "Development of Biochar-Based Functional Materials: Toward a Sustainable Platform Carbon Material," *Chemical Reviews*, **115**(22), 125-128(2015).
18. Li, C.-Z., "Some Recent Advances in the Understanding of the Pyrolysis and Gasification Behaviour of Victorian Brown Coal," *Fuel*, **86**(12), 1664-1683(2007).
19. Li, C.-Z., "Importance of Volatile-char Interactions During the Pyrolysis and Gasification of Low-rank Fuels-a Review," *Fuel*, **112**, 609-623(2013).
20. Joyce, J., Dixon, T. and Costa, J. C. D. D., "Characterization of Sugar Cane Waste Biomass Derived Chars from Pressurized Gasification," *Process Safety & Environmental Protection*, **84**(B6), 429-439(2006).
21. Lapuerta, M., Hernández, J. J., Pazo, A. and López, J., "Gasification and co-gasification of Biomass Wastes: Effect of the BioMass Origin and the Gasifier Operating Conditions," *Fuel Processing Technology*, **89**(9), 828-837(2010).
22. Matsuoka, K., Yamashita, T., Kuramoto, K., Suzuki, Y., Takaya, A. and Tomita, A., "Transformation of Alkali and Alkaline Earth

Metals in Low Rank Coal During Gasification," *Fuel*, **87**(6), 885-893(2008).
23. Song, H., Xiang, J., Sun, L., Xu, M., Qiu, J. and Peng, F., "Characterization of Char from Rapid Pyrolysis of Rice Husk," *Fuel Processing Technology*, **89**(11), 1096-1105(2008).
24. Li, D., Xu, G., Suda, T. and Murakami, T., "Potential Approaches to Improve Gasification of High Water Content Biomass Rich in Cellulose in Dual Fluidized Bed," *Fuel Processing Technology*, **91**(91), 882-888(2010).